LAWRENCE
LIVERMORE
NATIONAL
LABORATORY

LLNL-PROC-528333

Building an Efficient Model for Afterburn Energy Release

S. Alves, A. Kuhl, F. Najjar, J. Tringe, L. McMichael, L. Glascoe

February 10, 2012

82nd Shock and Vibration Symposium
Baltimore, MD, United States
October 30, 2011 through November 4, 2011

Disclaimer

Building an Efficient Model for Afterburn Energy Release

Steven Alves, Allen Kuhl, Fady Najjar, Joseph Tringe, Larry McMichael, Lee Glascoe
Lawrence Livermore National Laboratory

LLNL-PROC-528333

ABSTRACT

Many explosives will release additional energy after detonation as the detonation products mix with the ambient environment. This additional energy release, referred to as afterburn, is due to combustion of undetonated fuel with ambient oxygen. While the detonation energy release occurs on a time scale of microseconds, the afterburn energy release occurs on a time scale of milliseconds with a potentially varying energy release rate depending upon the local temperature and pressure. This afterburn energy release is not accounted for in typical equations of state, such as the Jones-Wilkins-Lee (JWL) model, used for modeling the detonation of explosives. Here we construct a straightforward and efficient approach, based on experiments and theory, to account for this additional energy release in a way that is tractable for large finite element fluid-structure problems. Barometric calorimeter experiments have been executed in both nitrogen and air environments to investigate the characteristics of afterburn for C-4 and other materials. These tests, which provide pressure time histories, along with theoretical and analytical solutions provide an engineering basis for modeling afterburn with numerical hydrocodes. It is toward this end that we have constructed a modified JWL equation of state to account for afterburn effects on the response of structures to blast. The modified equation of state includes a two phase afterburn energy release to represent variations in the energy release rate and an afterburn energy cutoff to account for partial reaction of the undetonated fuel.

DISCLAIMER

This work was supported by the Science and Technology Directorate, U.S. Department of Homeland Security (DHS/S&T).
This work performed under the auspices of the U.S. Department of Energy by Lawrence Livermore National Laboratory under Contract DE-AC52-07NA27344.

INTRODUCTION

Afterburn is combustion that occurs after an explosive is detonated. The detonation products mix and react with oxygen at high temperature and pressure, releasing a substantial amount of energy. The difference between the heat of combustion and the detonation energy for an explosive material generally indicates how much energy can be released through afterburn. For C-4, the heat of combustion is more than two times larger than the detonation energy, meaning that more energy can theoretically be released through afterburn compared to detonation. Afterburn can occur for both ideal and non-ideal explosives. For ideal explosives, the detonation reaction rate is very fast, occurring on the order of microseconds. The detonation reaction rate can be about an order of magnitude slower for non-ideal explosives, such as many home-made explosives (HMEs). While both ideal and non-ideal detonation energy is released on the order of tens to hundreds of microseconds, afterburn energy is released much slower, on a time scale of milliseconds. Temperature and pressure conditions can affect the release rate of afterburn energy, but even at optimum conditions afterburn is a much slower phenomenon than detonation. The fact that afterburn energy is released much slower than detonation energy and can be incomplete highlights the difficulty of how to measure the effect of afterburn on structural response.

It is of interest to have a bounding capability to assess the contribution of afterburn to structural loading, response and damage from an explosive event. However, the typical approach for representing blast in hydrocodes does not represent afterburn. The Jones-Wilkins-Lee (JWL) equation of state captures detonation energy release [1], but later time afterburn energy release is not captured. Thus, a modified JWL model has been developed that captures the general features of afterburn energy. The JWLa (JWL-afterburn) model that has been implemented in ALE3D [2] provides an efficient representation that allows for study of the effects of afterburn.

Barometric calorimeter tests have been performed with C-4 and two HMEs. The tests were performed in nitrogen and air atmospheres. The presence of oxygen in air causes afterburn, while the nitrogen environment is unreactive, thereby preventing afterburn. Comparison of tests in the two atmospheres isolates the significance of afterburn. Figure 1 illustrates the additional impulse that is delivered in air compared to nitrogen over 30 milliseconds. These tests provided data that have been used in order to assess the JWLa model.

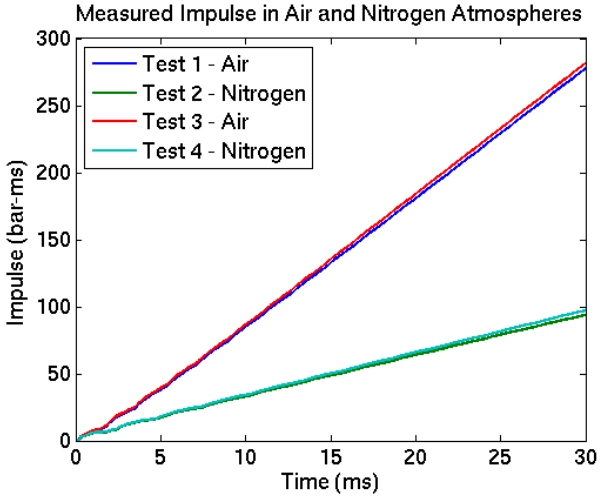

Figure 1. Specific impulse recorded from barometric calorimeter tests in air and nitrogen atmospheres

AFTERBURN MODEL

The JWL-afterburn (JWLa) model adds a time-dependent term to the standard JWL pressure calculation.

$$P_{JWLa} = P_{JWL} + \frac{E_{AB}}{v} Y_p(t) \tag{1}$$

In Eq. (1), v is the relative volume, E_{AB} is the afterburn energy, and $Y_P(t)$ defines the time dependence for the release of afterburn energy. The afterburn energy is determined by comparing results from a standard JWL simulation in a closed volume to a constant volume explosion calculation in Cheetah, which is a thermochemistry code for explosives [3]. The constant volume explosion in Cheetah includes the mass fraction of air available in the closed volume. The difference in final pressure between the standard JWL simulation and Cheetah run is computed, and the difference in pressure is converted to energy per unit volume of the explosive charge. The time dependence function has the form 1-exp(-t/ τ), where τ is the time constant for energy release. The time function allows for a two-stage release of energy with different rates. The two-stage release of energy accounts for the fact that near optimum conditions for combustion, very high pressure and temperature, will exist immediately after detonation, but as the pressure and temperature decrease the rate of combustion may slow. This phenomenon has been observed in combustion simulations by Kuhl et al [4]. The deviation from optimum conditions becomes more significant as the volume of the container is increased, so the two-stage release capability is likely important for open air blasts. The JWLa also has an option to cutoff before the entire afterburn energy is released. This accounts for situations when the full theoretical potential for afterburn may not be reached, because the conditions drop below the threshold for combustion to occur. Examples of the time function are shown in Figure 2 through Figure 4. Figure 2 shows the base function, Figure 3 demonstrates the two-stage option, and Figure 4 demonstrates the cutoff option.

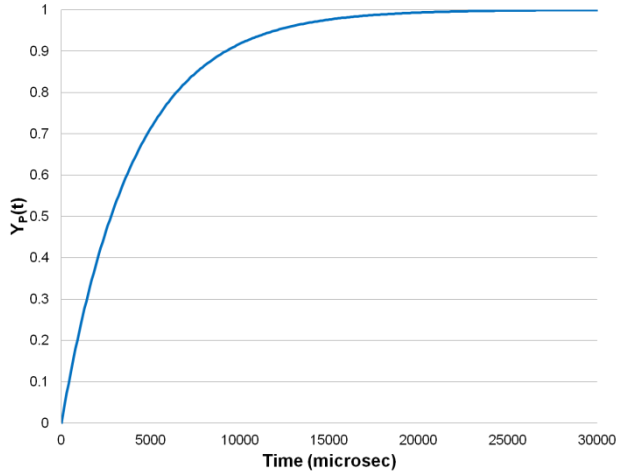

Figure 2. One-stage time function, time constant of 4000 microseconds

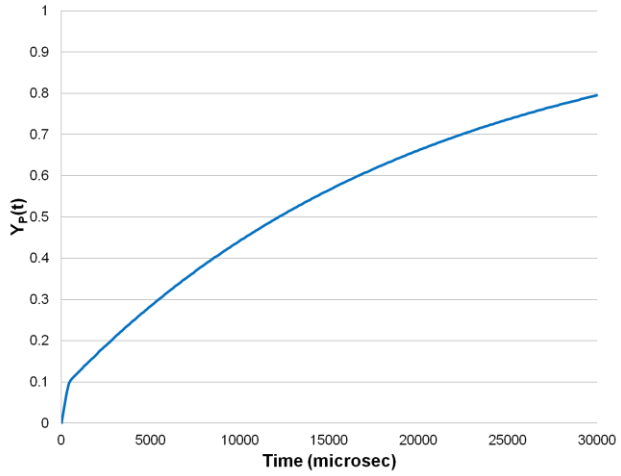

Figure 3. Two-stage time function, first stage time constant of 4000 microseconds, second stage time constant of 20000 microseconds, transitions at 10% of the total energy release

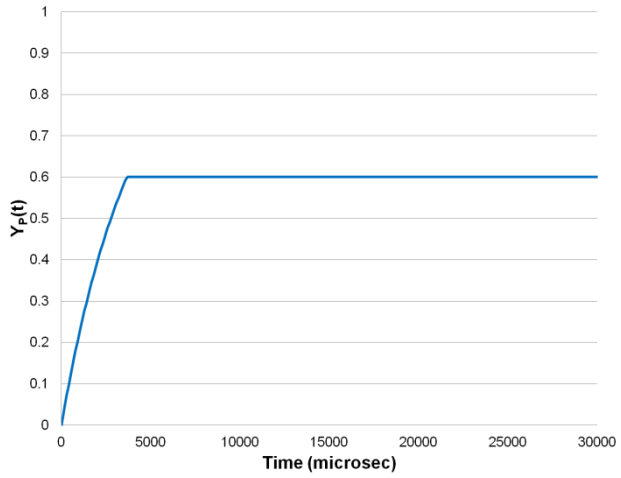

Figure 4. One-stage time function with energy cutoff at 60% of total, time constant of 4000 microseconds

In Cheetah [3], the total energy of detonation is separated into two components, the mechanical energy of detonation and the thermal energy of detonation. The mechanical energy of detonation is the energy available to do mechanical work as the volumetric expansion of the detonation products proceeds along the adiabat to its endpoint at a pressure of 1 atm. The thermal energy of detonation is the amount of energy locked up as heat in solid detonation products. It corresponds to the energy difference between the thermodynamic state at a pressure of 1 atm and a temperature of 298 K and the thermodynamic state at the adiabat endpoint. The total energy released during detonation is the sum of the mechanical and the thermal energy. While the mechanical energy is described as the amount of energy available to do work, it is generally the total energy of detonation that will be measured in a calorimeter. In general, the JWL model is based on the mechanical energy of detonation. Thus, in cases where the thermal energy of detonation is significant, the JWL model should underestimate the energy release that is measured at late times in the calorimeter even for a nitrogen atmosphere.

The afterburn energy that is added through the JWLa model is related to the heat of combustion of the explosive compared to the result with a JWL model. This means that the JWLa model can account for thermal energy of detonation assuming that the thermal energy can be represented in the same way as afterburn energy. Thus, the JWLa model should release the appropriate amount of energy for a calorimeter experiment in air. More investigation is necessary to determine how the thermal energy of detonation can affect structural response and whether the JWLa accounts for this in an appropriate manner.

BAROMETRIC CALORIMETER EXPERIMENT

The barometric calorimeter used for the experiments is a 506 liter cylindrical chamber. The cylinder has an internal diameter and height of 34 inches. The calorimeter is shown in Figure 5. Kuhl and Reichenbach [5] describe the concept of a barometric calorimeter in more detail. The atmosphere can be controlled inside the calorimeter, such that it is possible to perform explosive tests in air and nitrogen atmospheres. A hemispherical charge with a hemispherical booster was placed at the center of the calorimeter (Figure 6). The charge was detonated at the base of the booster. An ABS plastic shell with a Lexan base was used to contain particulate HMEs. Two different HMEs were tested. The same container was used for C-4 charges to maintain consistency.

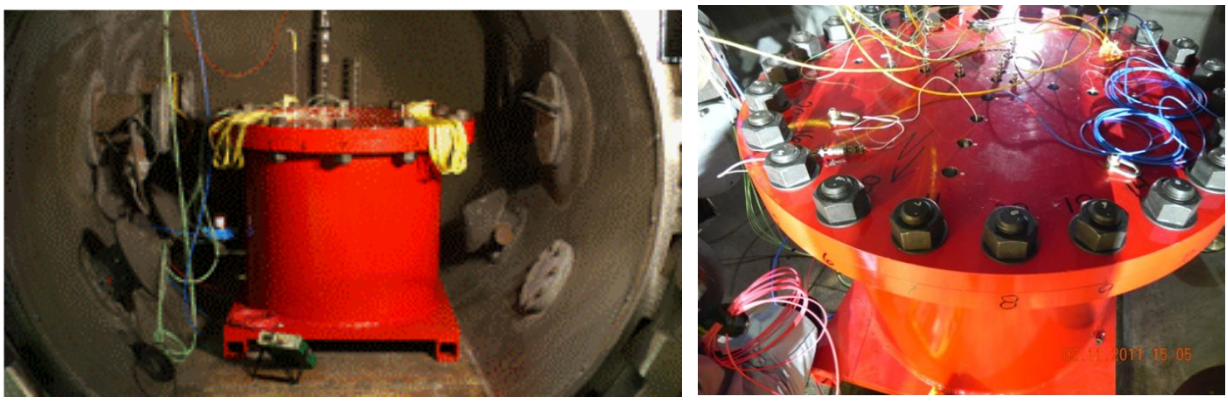

Figure 5. Barometric calorimeter

Figure 6. Charge placed at the center of the calorimeter (left), charge and booster inside ABS plastic shell (right)

The calorimeter was instrumented in the lid with piezoelectric and piezoresistive pressure gauges. The lid has a standoff of 17 inches from the bottom of the charge, and the pressure gauges are placed at ground ranges of 0 inches to 12 inches. A ground range of 0 inches is directly above the charge, and the other ground ranges extend radially on the lid. Data from the pressure gauges provide a means for comparing the blast pressures with and without afterburn occurring. Thermocouples and optical fibers were also installed in the lid, but the pressure data are the focus of this work. Pressure histories from the calorimeter lid for four C-4 tests, two in air and two in nitrogen, are shown in Figure 7. The figure illustrates that within 3 milliseconds after detonation the effects of afterburn are apparent, because the recorded pressure in air (tests 1 and 3) is higher than the recorded pressure in nitrogen (tests 2 and 4).

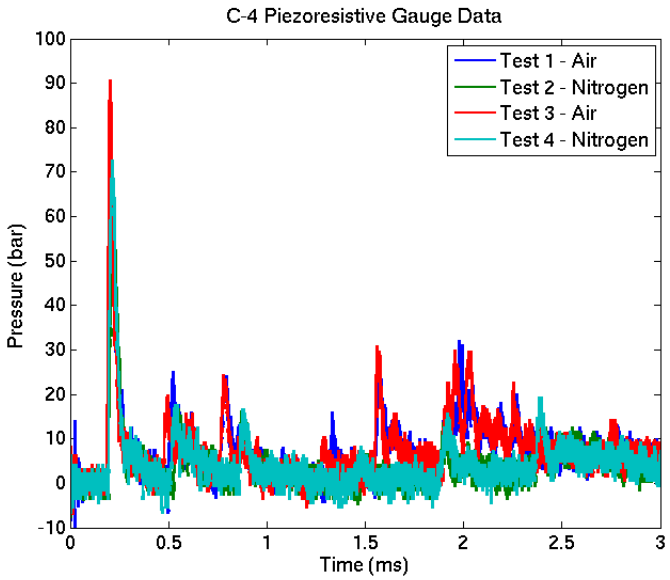

Figure 7. Pressure histories recorded for four C-4 tests, two in air and two in nitrogen (8-inch ground range)

MODELING OF THE EXPERIMENT

A model of the barometric calorimeter was generated for ALE3D (Figure 8). Both the explosive and the booster are modeled, and as in the tests the charge is detonated at the base of the booster. The explosives are modeled using both the standard JWL model and the modified JWLa model. The JWL model represents an explosive in a nitrogen atmosphere, excluding the potential effect of thermal energy of detonation. The JWLa model represents an explosive in an air atmosphere. For the JWLa representations, a time constant of approximately 4 milliseconds is used and the energy is released in a single stage with no cutoff (see Figure 2). The rationale for this is that the calorimeter is a relatively small enclosed volume, so the conditions for combustion will be at or near optimum conditions for the duration of the experimental time scale. Simulated pressure histories collected on the lid of the calorimeter demonstrating the effect of utilizing the JWLa model are shown in Figure 9. The figure demonstrates that the effect at early time is not very significant, but the contribution from the afterburn starts to become more significant around 1.5 milliseconds after detonation.

Figure 8. ALE3D model of the barometric calorimeter in half-symmetry

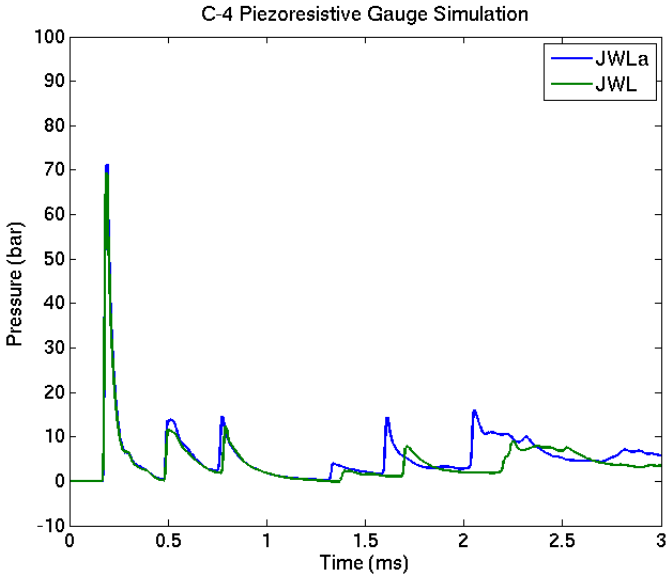

Figure 9. Simulated pressure histories using the JWL and JWLa models (8-inch ground range)

The simulations have been compared to the experimental records for both the early time and late time regimes. Early time means the first few hundred microseconds, and it covers the first positive phase of the blast pressures. This assesses the initial effects of the blast loads. Late time means several tens of milliseconds, and this assesses the total amount of energy released.

C-4 MODELING

For the early time comparisons, simulated pressure histories have been compared to several piezoelectric pressure gauge records for ground ranges between 0 inches and 12 inches. The specific impulse is determined by integrating the pressure history over time. Comparisons of the specific impulse up to 400 microseconds after detonation for the C-4 experiments and simulations are shown in Figure 10. The duration of 400 microseconds was chosen to capture the positive phase at all ground ranges without contribution from reflections. Figure 11 through Figure 13 provide comparisons of test recordings with simulated pressures and impulses. Time zero in the figures is the detonation time. Note that a reflection is apparent in Figure 13 at about 450 microseconds. This reflection is only visible in Figure 13 because the ground range of 10 inches is closer to the wall of the calorimeter. In the tests, the air atmosphere increased the specific impulse by about 12% on average, but in the simulations the JWLa model only increased the impulse by about 3%. Despite this difference, it can be seen from the figures that the simulations capture the pressure and impulse from the blast experiments quite well, because the presence of afterburn does not have a significant effect on the first positive phase of blast pressures. Figure 14 and Figure 15 demonstrate that the JWLa model does not release significantly more energy than the JWL model in the first few hundred microseconds.

It is of note in Figure 10 that the pressure records at a ground range of 0 inches demonstrate a significant scatter. This is believed to be from jetting due to Rayleigh-Taylor instabilities. The simulations do not exhibit this affect because the mesh resolution is not fine enough to capture the instabilities. One other feature that the reader may notice is that the impulses recorded at 4 inches, 8 inches, and 12 inches exhibit a visibly larger trend with ground range than the other ground ranges. It is believed that this is due to reflections off of the mounting post (see Figure 6) used to support the charge prior to detonation, because those three pressure gauges were placed in line with the post. The simulations also capture the effect of the post.

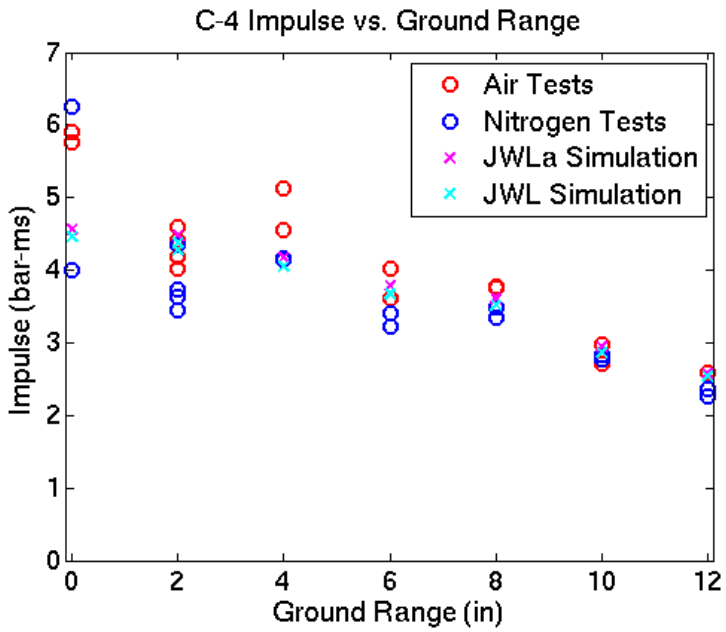

Figure 10. Early time specific impulse compared between C-4 experiments and simulations for ground ranges on the lid up to 12 inches, impulse computed up to 400 microseconds

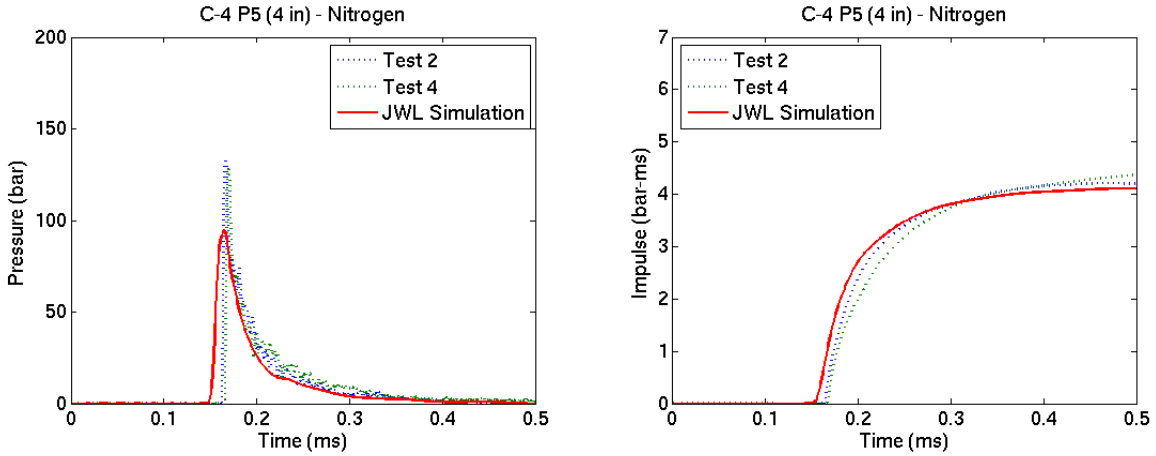

Figure 11. Pressure and specific impulse comparisons of C-4 tests in nitrogen atmosphere and JWL simulation at ground range of 4 inches

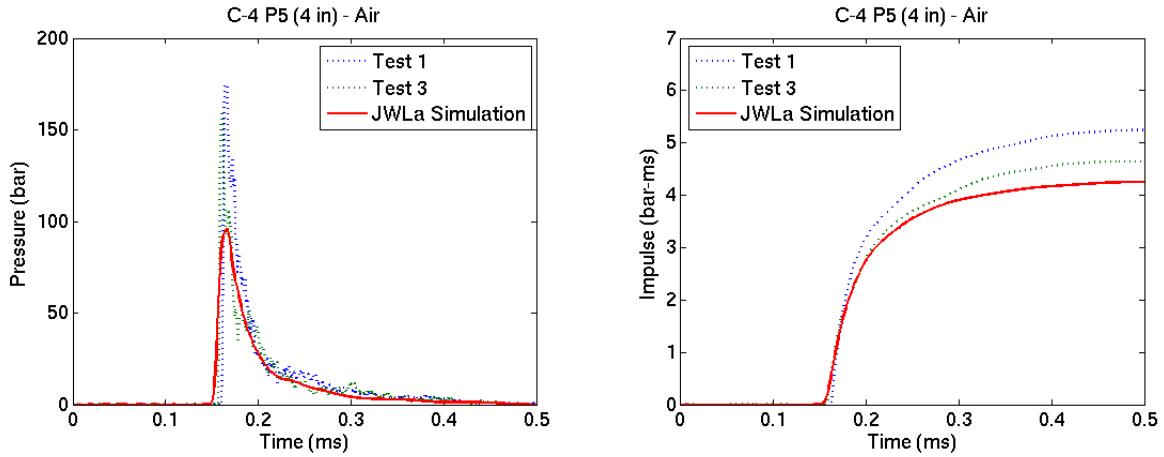

Figure 12. Pressure and specific impulse comparisons of C-4 tests in air atmosphere and JWLa simulation at ground range of 4 inches

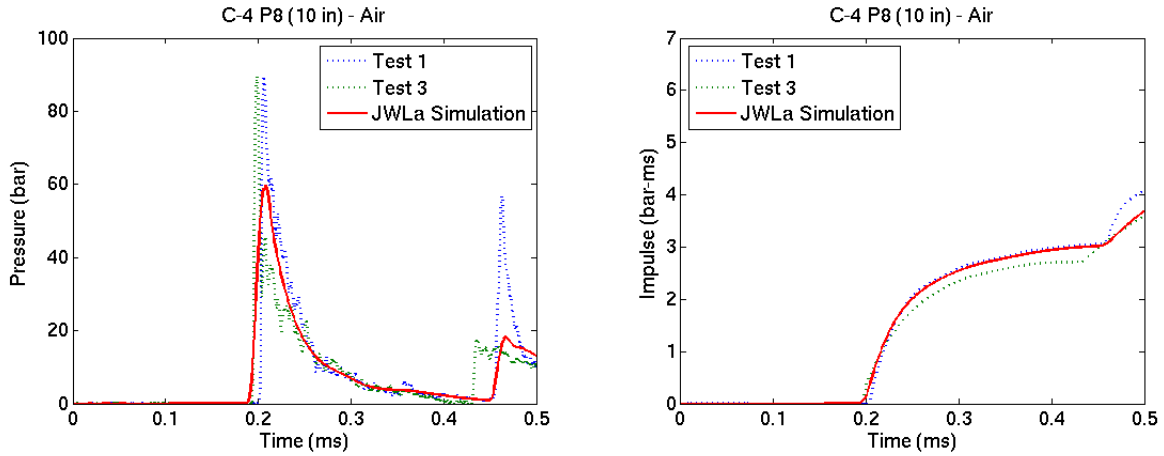

Figure 13. Pressure and specific impulse comparisons of C-4 tests in air atmosphere and JWLa simulation at ground range of 10 inches

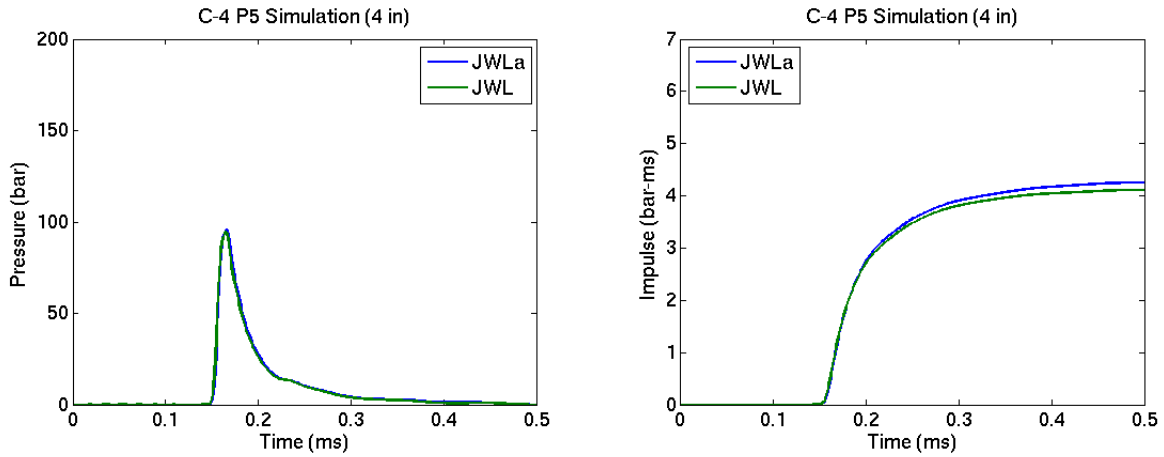

Figure 14. Pressure and specific impulse comparisons of C-4 simulations at ground range of 4 inches

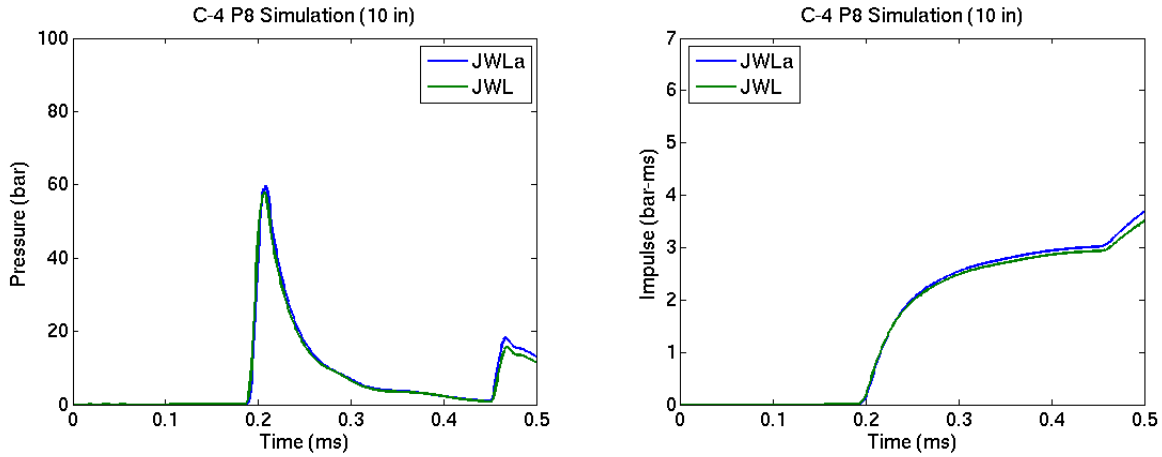

Figure 15. Pressure and specific impulse comparisons of C-4 simulations at ground range of 10 inches

For the late time comparisons, the ambient pressure between 20 and 30 milliseconds is determined from the simulations and compared to a piezoresistive gauge in the lid. The simulated pressure is recorded at the same location in the lid as in the experiment. The averages from the tests are compared to simulated values in Table 1. The theoretical values obtained from a Cheetah constant volume explosion are also provided in the table for both nitrogen and air atmospheres. The pressures are reported as gauge pressure, so the values are the change in pressure relative to atmospheric pressure. The significant increase in pressure between nitrogen and air atmospheres indicates that while the afterburn does not significantly affect the energy release for the first arrival of blast pressures, the afterburn is a significant contribution to the total energy released.

Table 1. Change in pressure for C-4 in nitrogen and air atmospheres

	ΔP (bar)	
	nitrogen	air
Theoretical (Cheetah)	3.58	7.74
Average from tests	3.05	9.74
ALE3D model	3.43 (JWL)	7.40 (JWLa)

The nitrogen atmosphere and JWL model demonstrate reasonable agreement with each other and the theoretical Cheetah prediction. The smaller value from the tests can possibly be attributed to a detonation that was not completely efficient. Figure 16 demonstrates how well the JWL simulation agrees with the nitrogen atmosphere tests up to 3 milliseconds after detonation. The arrivals for the reflected waves are captured by the simulation, but it is apparent that the waves travel slightly faster in the simulation. This indicates that the wave speed of the model representing the nitrogen is slightly overestimated.

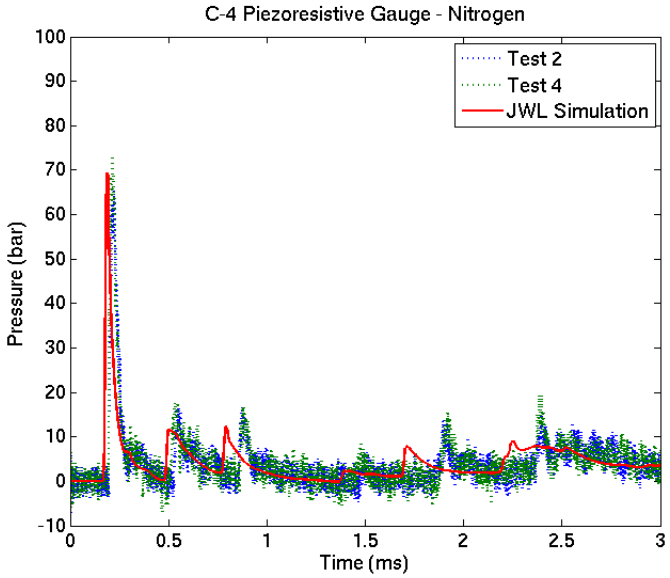

Figure 16. Pressure histories for C-4 in nitrogen atmosphere compared to JWL simulation to 3 milliseconds (8-inch ground range)

For the air atmosphere, the Cheetah prediction and JWLa model significantly underestimate the experimental value. The main reason for the late time discrepancy in air is believed to be the presence of the plastic shell and base used to hold the charge. Assuming that only about 2% of the available plastic combusts increases the simulated change in pressure from 7.40 bar to 9.56 bar, which is much more consistent with the experimental value of 9.74 bar. It was also determined that reducing the time constant from 4 milliseconds to approximately 2 milliseconds provides better agreement with the experiment with respect to impulse. This is demonstrated in Figure 17, which shows the specific impulse out to 30 milliseconds after detonation for both air and nitrogen atmospheres. The figure shows the good agreement of the JWL simulation with the nitrogen tests, but it also demonstrates that the base case for the JWLa simulation without considering combustion of plastic significantly underpredicts the impulse. When the combustion of the plastic is considered, the impulse agrees much better with the experiment, but the simulation still lags slightly. When the time constant is reduced by a factor of two, the agreement improves even more. Figure 18 shows the comparison of the JWLa simulations with the air tests, and the agreement is similar to what was observed for nitrogen in Figure 16. With the reduced time constant, as with the nitrogen atmosphere, the waves travel slightly faster in the simulation than the tests. It is also of note that when the reduced time constant is used and plastic combustion is considered, the JWLa simulations yield a positive phase impulse over the first 400 microseconds that increases 6% on average compared to the JWL simulations. This is more consistent with the 12% increase from the experiments.

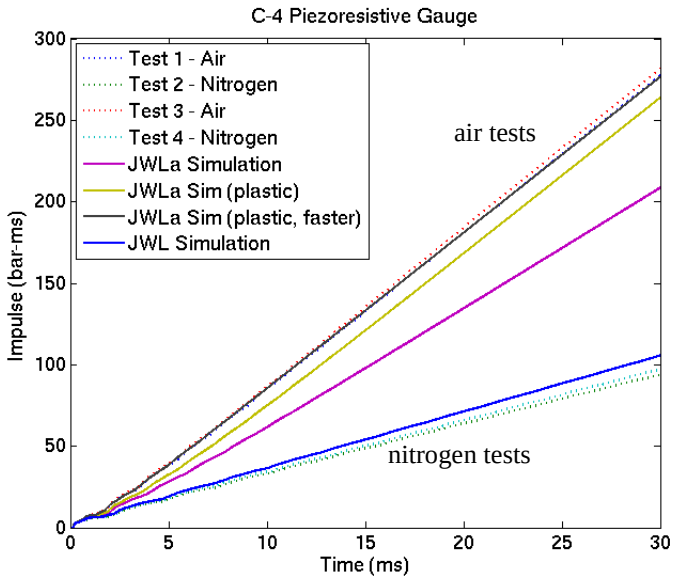

Figure 17. Specific impulse for C-4 out to 30 milliseconds for nitrogen and air atmospheres compared to JWL simulation and three JWLa simulations: base case, additional combustion of plastic, and additional combustion of plastic with a faster time constant of about 2 milliseconds

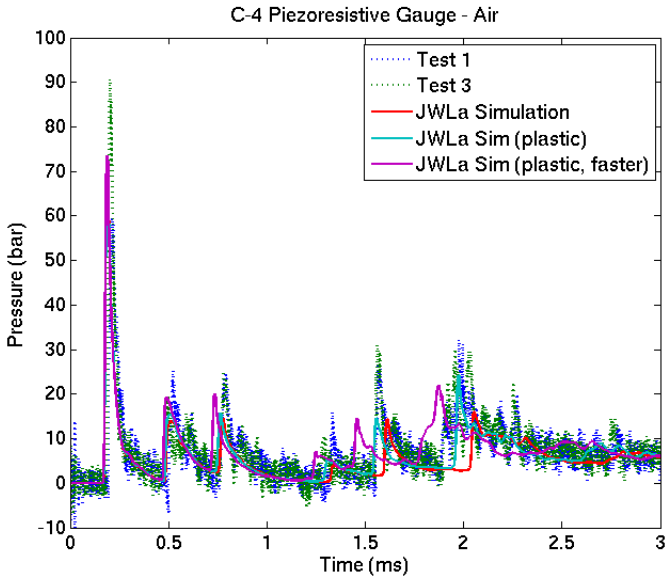

Figure 18. Pressure histories for C-4 in air atmosphere compared to JWLa simulations to 3 milliseconds: base case, additional combustion of plastic, and additional combustion of plastic with a faster time constant of about 2 milliseconds (8-inch ground range)

HME MODELING

Two HMEs were used in the tests, and these materials are designated as HME 1 and HME 2. HME 1 has a substantial potential for afterburn, but HME 2 is fuel-lean so there is no theoretical potential for afterburn. Table 2 and Table 3 give the late time pressure comparison between theory, testing and modeling for HME 1 and HME 2, respectively. Notice that the theoretical Cheetah values are identical in nitrogen and air for HME 2. As in the C-4 tests, the blasts in nitrogen do not achieve the pressure change that is predicted by Cheetah. This again indicates that

the detonation was probably not fully efficient for either material. Also, as for C-4, the tests in air were underpredicted by Cheetah and ALE3D, which is again most likely due to the combustion of the plastic container.

Table 2. Change in pressure for HME 1 in nitrogen and air atmospheres

	ΔP (bar)	
	nitrogen	air
Theoretical (Cheetah)	3.65	6.30
Average from tests	2.59	8.29
ALE3D model	2.09 (JWL)	6.59 (JWLa)

Table 3. Change in pressure for HME 2 in nitrogen and air atmospheres

	ΔP (bar)	
	nitrogen	air
Theoretical (Cheetah)	2.97	2.97
Average from tests	2.38	4.17
ALE3D model	1.03 (JWL)	3.02 (JWLa)

Unlike the C-4 modeling, the JWL model for both HMEs significantly underpredicts the change in pressure measured from the tests in nitrogen. It is believed that this discrepancy is due to the fact that the JWL does not account for thermal energy of detonation, and these HMEs have solid detonation products that contribute thermal energy. As was discussed earlier, the thermal energy of detonation is part of the total energy of detonation that is measured in a calorimeter.

The effects of afterburn for HME 1 on the earlier time arrival of blast waves are illustrated in Figure 19 and Figure 20. Note that the positive phase is captured by 450 microseconds for this explosive, which is longer than the C-4 duration of 400 microseconds because the waves from the HME travel slower. Recall that the tests include combustion of the plastic container, but the JWLa modeling does not include the contribution from the plastic. The figures demonstrate that the HME 1 afterburn effect is more significant than C-4 in the early time. The air environment increases the first positive phase impulse by 19% on average. The JWLa model yields an increase of 7% on average, which is likely lower than the experimentally observed value due to the contribution from combustion of plastic that skews the experimental results. Notice in Figure 20 that the second peak in the experimental data occurring at about 500 microseconds after detonation has a magnitude similar to the first peak, particularly in the air tests (numbers 1 and 3). This peak is from a reflection, but it is not known why the magnitude is so large. It is possible that this is related to the fact that HMEs often do not undergo ideal detonation so the release of energy is a slower process.

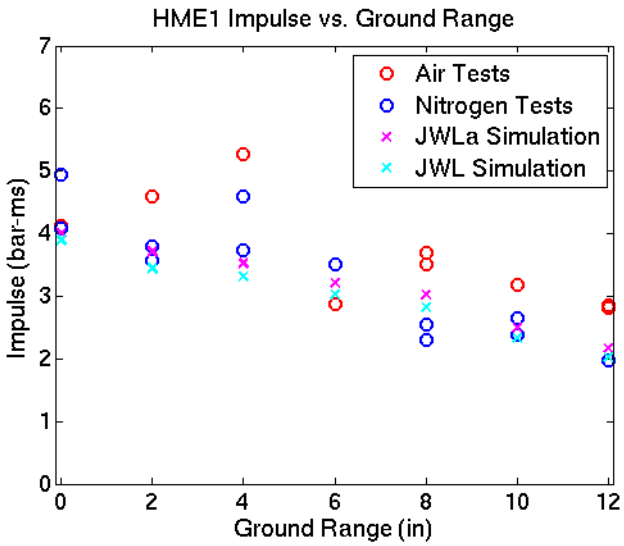

Figure 19. Specific impulse compared between HME 1 experiments and simulations for ground ranges on the lid up to 12 inches, impulse computed up to 450 microseconds

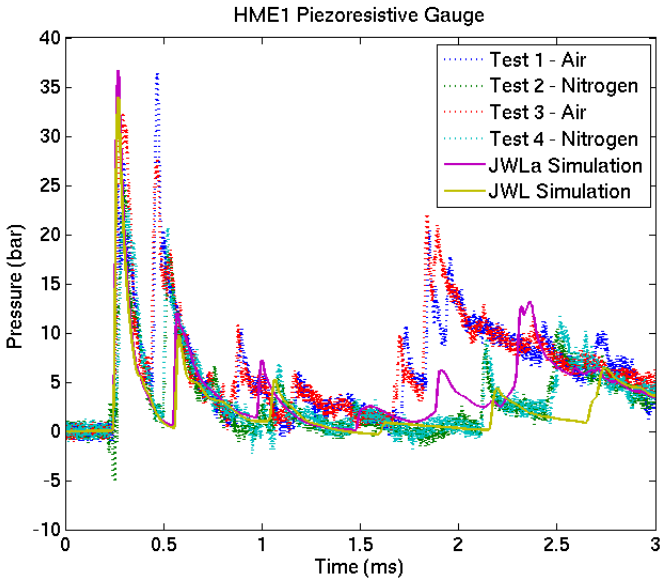

Figure 20. Pressure histories for HME 1 in nitrogen and air atmospheres compared to JWL and JWLa simulations to 3 milliseconds (8-inch ground range)

The effects of combustion of plastic in the HME 2 tests are illustrated in Figure 21 and Figure 22. Again, note the longer duration of 550 microseconds for capturing the positive phase for this HME. The test may actually exhibit some explosive afterburn in air because fuel may remain after an incomplete detonation. The increase in positive phase impulse is only 7% on average for HME 2. It makes sense that this is lower than the C-4 and HME 1 tests, since the explosive itself has no theoretical potential for afterburn. The JWLa simulation actually adds energy that represents the thermal energy of detonation, and this increases the positive phase impulse by 6% on average. In Figure 22, the improved agreement that the JWLa simulation attains with the test in nitrogen indicates that accounting for thermal energy of detonation using the same approach that was formulated to account for afterburn energy may be appropriate, but more study is necessary to further investigate this.

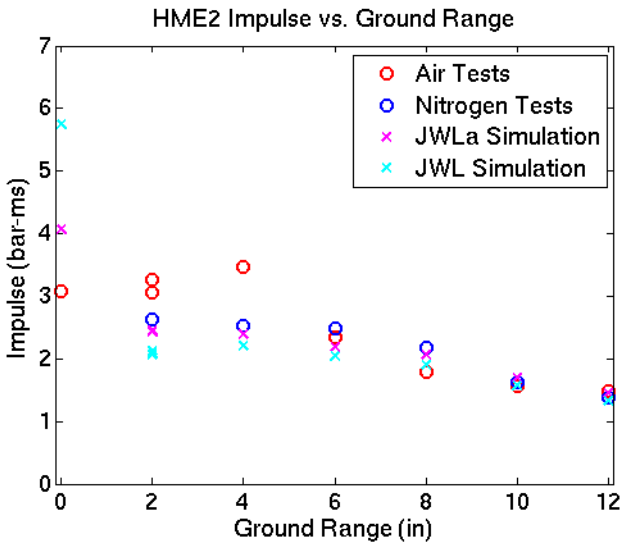

Figure 21. Specific impulse compared between HME 2 experiments and simulations for ground ranges on the lid up to 12 inches, impulse computed up to 550 microseconds

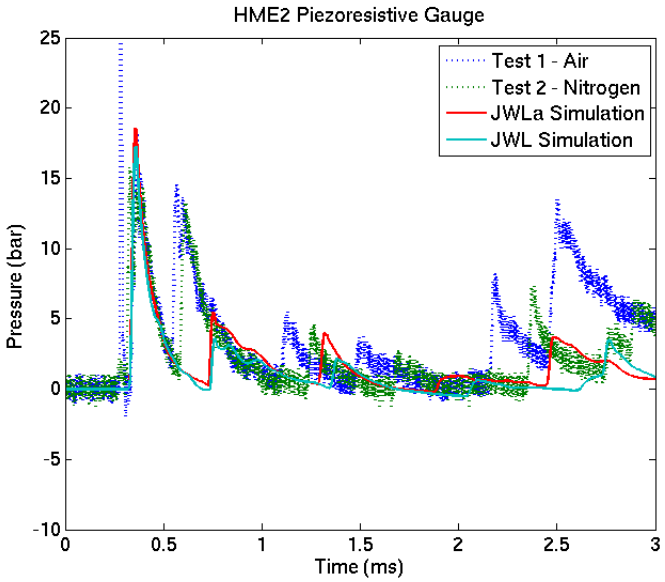

Figure 22. Pressure histories for HME 2 in nitrogen and air atmospheres compared to JWL and JWLa simulations to 3 milliseconds (8-inch ground range)

CONCLUSIONS

A modified JWL model for afterburn, termed the JWLa, has been implemented in ALE3D providing an efficient approach to approximate the effects of afterburn in a blast simulation. The JWLa model releases additional energy after detonation on the time scale of milliseconds. This model provides a capability to investigate and bound the importance that afterburn may have in a structural damage assessment.

Barometric calorimeter experiments with C-4 and two home-made explosives provided blast pressure data that were compared to simulations with the JWLa model. In both the experimental results and the simulations there is little affect from afterburn in the first several hundred microseconds, but the impulse delivered over tens of milliseconds is increased on the order of two to three times by afterburn. The test setup included a plastic container for the charge

that appears to have significantly affected the results by providing additional fuel for combustion, but comparisons between the experiments and simulations still provide confidence that the JWLa model can reasonably represent afterburn for the purpose of structural damage assessments. The approach for computing afterburn energy delivers an additional impulse to a structure that is consistent with the magnitude measured in the experiments. The timing for the energy release in the model also appears to be realistic. While the exact value of the time constant is uncertain, the original value that was assumed yielded a reasonable approximation of the test results.

It appears that the JWLa model may also be able to represent thermal energy of detonation in a calorimeter. More study is necessary to understand whether this phenomenon can affect structural response and to what degree.

Additional barometric calorimeter experiments are planned that will remove most of the non-explosive combustible materials. This testing will include C-4 and HMEs. These experiments will help to assess and further refine the modeling approach.

ACKNOWLEDGEMENTS

The authors would like to thank Laura Parker and Doug Bauer of the Department of Homeland Security's Science and Technology Directorate for their sponsorship and assistance in these efforts.

REFERENCES

1. Lee, E. L., H. C. Hornig, and J. W. Kury, *Adiabatic Expansion of High Explosive Detonation Products*, UCRL-50422, Lawrence Radiation Laboratory, University of California, Livermore, May 1968.
2. Nichols III, A. L., ed., *User's Manual for ALE3D, An Arbitrary Lagrange/Eulerian 2D and 3D Code System, Volumes 1 and 2*, Version 4.14.x, LLNL-SM-471671, Lawrence Livermore National Laboratory, March 2011.
3. Bastea, S., L. E. Fried, K. R. Glaesemann, W. M. Howard, I-F. W. Kuo, P. C. Souers, P. A. Vitello, *Cheetah 6.0 User's Manual*, LLNL-SM-416166, Lawrence Livermore National Laboratory, May 2010.
4. Kuhl, A. L., A. K. Oppenheim, R. E. Ferguson, H. Reichenbach, and P. Neuwald, *Effects of Confinement on Combustion of TNT Explosion Products in Air*, UCRL-JC-137418, Lawrence Livermore National Laboratory, February 2000, submitted to 28th International Symposium on Combustion.
5. Kuhl, A. L., and H. Reichenbach, *Barometric Calorimeters*, Russian Journal of Physical Chemistry B, Vol. 4, No. 2 (2010), pp. 271-278.